JOURNAL OF APPLIED ENGINEERING SCIENCES
ISSN: 2247-3769 / e-ISSN: 2284-7197
sciendo
VOL. 13(26), ISSUE 2/2023
ART.NO. 386 pp. 281-288

NUMERICAL STUDY ON THE SEISMIC PERFORMANCE OF HYBRID SHEAR WALLS WITH CENTERED OPENINGS

V. Todea [a], *, D. Dan [a], S.C. Floruț [a], V. Stoian [a], V.Ș. Popescu [a]

[a] Faculty of Civil Engineering, Politehnica University Timisoara, 2nd T. Lalescu, 300223 Timisoara, Romania
E-mails: * viorel.todea@upt.ro, daniel.dan@upt.ro, codrut.florut@upt.ro, valeriu.stoian@upt.ro, serban.popescu@student.upt.ro

Received: 14.08.2023 / Accepted: 15.09.2023 / Revised: 18.09.2023 / Available online: 15.12.2023

DOI: 10.2478/jaes-2023-0036

KEY WORDS: Hybrid walls, Shear studs, Numerical modelling, Seismic behavior

ABSTRACT:

The lateral resisting system comprised of hybrid shear walls is often met nowadays for high rise buildings, to reduce the lateral displacements of the building during a seismic event and to limit the damages of non-structural elements. In fact, "hybrid shear walls" term will replace the old terminology used for composite steel concrete shear walls. This structural system develops a very stable seismic behavior under cyclic lateral loads, but the seismic performance of the system could be significantly changed by the openings required for architectural or functional reasons. This paper presents in detail the seismic behavior of a composite steel-concrete shear wall designed with centered openings and partially embedded steel profiles in the edges. The composite wall was subjected to vertical and horizontal loads and tested to full failure using a cyclic loading testing procedure that simulated the action of an earthquake, aiming to record the seismic performance of the wall in terms of bearing capacity, deformation capacity, failure mode and stiffness degradation. The low-dissipative behavior recorded experimentally of the tested specimen was afterward validated and assessed in detail by performing numerical analyses using ATENA 3D Engineering software. The numerical results were extended to investigate furthermore other structural solutions to increase the bearing capacity and the seismic performance of the wall. It was found that a significant increase in deformation capacity could be obtained if the wall coupling beams are reinforced by diagonal steel bars or additional steel plates.

1. INTRODUCTION

During the last decades an extensive work has been performed to study the seismic behaviour of the composite steel-concrete shear walls. By embedding steel profiles in the concrete core of the reinforced concrete walls, a great deformation capacity and flexural stiffness compared to the conventional reinforced concrete walls is attained (Dan, 2011). Beside their seismic performance, the composite shear walls present other structural advantages as: reduced thicknesses, multiple possibilities to connect the walls with steel or composite frames, a reduced construction erecting time or costs by using prefabricated steel profiles. In the existing literature different types of composite steel-concrete shear walls were experimentally and theoretically investigated: isolated walls (Olabi, 2021; Kisa, 2021) or coupled shear walls (Li, 2019) both systems developing a great seismic performance. By coupling the isolated piers with horizontal beams, the overall seismic performance of the system is influenced by the hysteretic resistance of the coupling beams or by the geometric position of the openings (Zhang, 2021; Liu, 2023). Nevertheless, the energy dissipation capacity is much higher for this type of structural walls in comparison with other structural systems. The axial compression ratios, the strength of concrete in compression or the steel ratios embedded in the edges of the walls, are other parameters that present a significant impact over the hysteretic performance of composite steel-concrete shear walls, as Hu et al. (Hu, 2021) and Labibzadeh et al. (Labibzadeh, 2021) recorded in their research. In many studies found in the literature, the influence of these parameters on the seismic behaviour of the structural walls is investigated by performing numerical analyses besides the experimental tests, using finite element method and software's. Zhen-bang Ma et al. (Ma, 2023) by performing a nonlinear finite element analysis on the seismic behaviour of one 1:4 scaled five-story SPRC composite wall coupled to steel side columns and designed with a plastic coupling ratio of 0.45, recorded that an excellent deformation capacity and a great energy dissipation capacity of the system could be obtained if a moderate value of 0.15 for the axial ratio is respected and the steel plate ratio embedded in the concrete core of the wall is 6.6%. Hyeon-Jin Kim et al. (Kim, 2023) studied the flexural performance of a new steel-concrete composite wall with boundary steel-U sections and conducted a parametric study using ATENA finite element software (Cervenka, 2017) to investigate the effect of axial force on the flexural capacity of the wall. The authors recorded that the maximum flexural capacity of the wall was attained when the axial compressive ratio was 30%. Yiwen Wu et al. (Wu, 2023) performed a numerical simulation and a parametric analysis to consider the influence of the aspect ratio, height-thickness ratio, and stiffness ratio on the hysteretic performance of six diagonally stiffened stainless steel plate shear walls subjected to low cyclic loading.

* Corresponding author: Viorel Todea, Research Assistant PhD Eng., Faculty of Civil Engineering, Politehnica University Timisoara, 2nd T. Lalescu, 300223 Timisoara, Romania, e-mail: viorel.todea@upt.ro

The authors indicated that the height to thickness ratio is the key factor that significantly affecting the energy dissipation of the walls. Jiuyang Li et al. (Li, 2022) investigated in detail using ABAQUS software the load-bearing performance of concrete shear walls with U-shaped sections. Yanqing Fu et al. (Fu, 2022) carried out a parameterized analysis on the key factors that are affecting the prefabricated new type studied SRC shear wall, including axial compression ratio, concrete strength grade, steel ratio of edge concealed columns, reinforcement ratio of vertical rebar section and thickness of the connecting plate. Based on the numerical study, it was recorded that the increase of axial compression ratio, the concrete strength grade or steel ratio of edge concealed column enhanced the bearing capacity of the new type prefabricated SRC shear wall, but at the same time also reduced the level of walls ductility. The authors consider that the steel ratio of the edge concealed columns must be greater than 7% if high concrete strength grades are used for such walls. Based on the previous studies, it can be concluded that by considering different simplified approaches to simulate the nonlinear behaviour of the constitutive materials or different finite element types and meshes to model the nonlinear behaviour of the reinforcements or macroelements, an increased accuracy of the tests results could be obtained numerically to study in detail the seismic behaviour of composite steel-concrete shear walls (Phan 2022; Javadi 2023; Zhang 2022). In this study the seismic performance of one composite steel-concrete shear wall with centred openings named CSRCW-21-CO is investigated experimentally and numerically. The specimen was designed and constructed at reduced 1:3 scale with partially I-shaped steel profiles embedded in the edges. The main objective of the research is to study the seismic performance of the wall subjected to vertical and lateral loads and to perform a numerical analysis using ATENA 3D Engineering software. The experimental results in terms of bearing capacity, hysteretic performance, deformation capacity, or stiffness degradation are detailed and presented over the chapters. The boundary conditions, the material laws and the numerical model considered in the numerical analyses and used to calibrate the numerical results are also described in this study.

2. DETAILS OF THE INVESTIGATED SPECIMEN

2.1 Specimen design

The investigated specimen is represented by a composite steel-concrete shear wall with I-shaped steel profiles partially embedded in the edges. A general perspective of the wall can be seen in Figure 1. The specimen measure over the encasement level in the beam foundation the total height of 3000 mm, the width of 1000 mm, and the thickness of 100 mm, simulating at 1:3 scale the first three stories of a building. Due to architectural requirements, in the proposed specimen centred rectangular openings with the dimension of 300x700 mm were considered in the design process of the wall. The openings follow the dimension of a regular door opening which measure at full scale the dimension of 700 x 2100 mm. The partially I-shaped steel profiles embedded in the edges of the specimen were manufactured using welded steel plates with the thickness of 5,65 mm and were connected with the web panel of the wall by a series of shear connectors those were designed as horizontal stiffeners perforated by two circular holes through two longitudinal bars were passing the entire length of the profiles. The cross-section arrangement of the wall vertical piers is presented in Figure 2 and the geometry of the shear connectors in Figure 3. The horizontal coupling beams between the vertical openings have the ratio length/height equal to one and were designed with rectangular cross section neglecting the contribution of a reinforced concrete slab as can be observed in Figure 4. Rebars of 8 mm diameter were used to reinforce the piers and the coupling beams of the specimen.

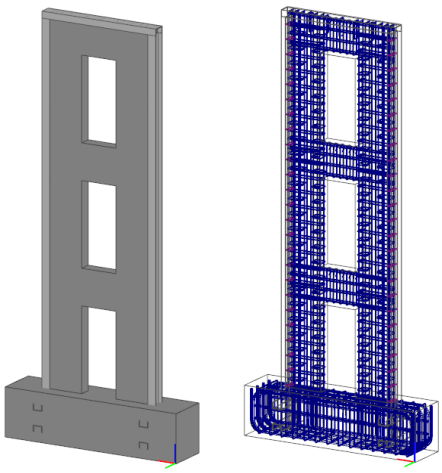


Figure 1. General perspective of the investigated specimen

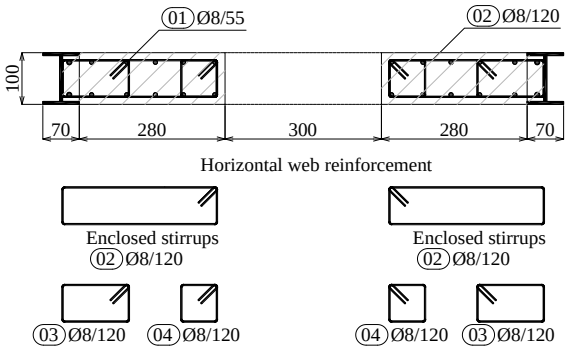


Figure 2. Cross section arrangement of the vertical piers

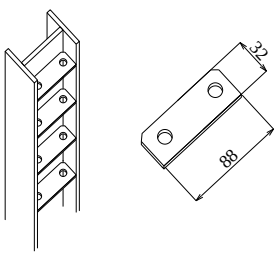


Figure 3. Details of embedded I-shaped steel profiles

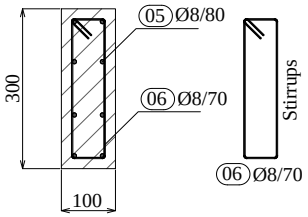


Figure 4. Cross section arrangement of the coupling beam

2.2 Materials

The specimen was designed with a concrete strength class of C30/37. The mean characteristic strength in compression for concrete result $f_{cm,cube}$=49,23 MPa based on three cubic samples tested in compression at 28 days.. Standard hot-rolled steel bars with ribbed periodical sections B500 with the ductility class C were used to reinforce the concrete web panel of the wall. The reinforcements were characterized by the following mechanical properties: yield strength f_{yk}=530,25 MPa and tensile strength f_u=636,02 MPa properties that were determined by performing tensile tests on three steel samples. The weldable steel plates used to construct the I-shaped steel profiles embedded on the edges of the wall and were hot-t-rolled S460 steel grade.

2.3 Test setup and loading strategy

The seismic behaviour of the specimen was monitored and recorded until the failure occurred. The local damages and the cracks propagation were recorded on each step of loading. The specimen was subjected in-plane to vertical and quasi-static horizontal forces simulating the effect of an earthquake. The horizontal forces were applied alternatively left-right following a load testing protocol (Figure 5). The vertical and horizontal forces were applied to the specimen by using two hydraulic jacks and one hydraulic press. The hydraulic jacks were mounted on two triangular frames at 400 mm distance below the upper part of the wall. The stand setup designed for the experimental test is sketched in Figure 6.

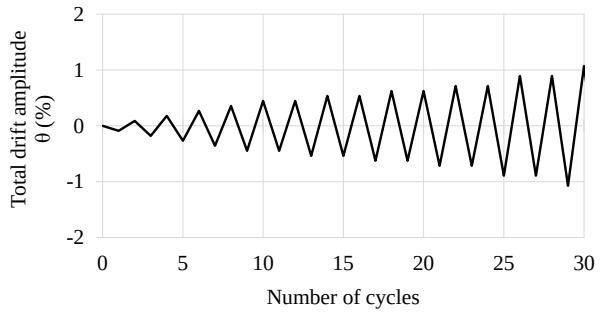


Figure 5. Load testing protocol

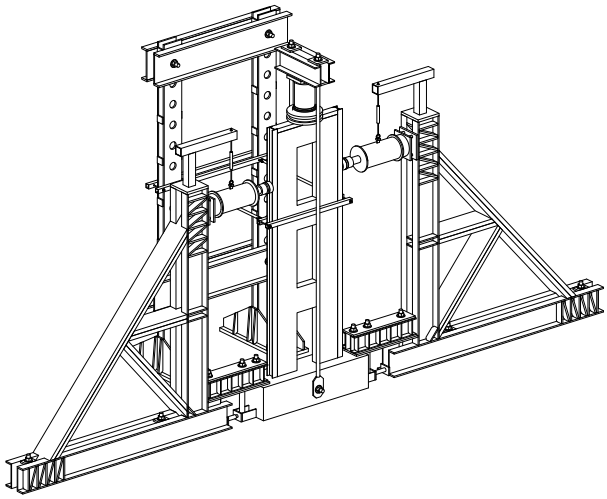


Figure 6. Experimental test setup

To simulate the gravitational loads acting on the specimen, a vertical compression force of 100 kN intensity was applied using the hydraulic cylinder that was positioned on the top of the wall and maintained constant during the experimental test by using a pair of pinned steel rods anchored into the beam foundation. The axial ratio computed based on the Eurocode 4 provisions (Eurocode 4, 2004) was ν_d=0,036. The experimental test was performed in displacement control mode. The lateral displacements of the wall were recorded by using a set of displacement transducers. The total drift amplitude denoted θ (%) which define the deformation capacity of the wall, was computed by the difference in displacements recorded between the top and the bottom displacement transducers, relative to the height of the wall. The out of plane translations of the wall were successfully restrained using a pinned horizontal frame attached on the specimen. Also, the translations of the beam foundation in plane of the wall were restrained by using steel bolts and some metallic subassemblies as can be seen in Figure 6.

3. EXPERIMENTAL RESULTS

3.1 Damages and cracks development

During the experimental test, the local damages, the lateral deflections, and the cracks propagation were recorded on each step of lateral loading. In Figure 7 the development of the cracks on the reinforced concrete web panel of the wall in the first step and at ultimate loading stage is illustrated. As can be seen, on both loading directions, first cracks were localized in the edges of the reinforced concrete coupling beams. The cracks were oriented towards the horizontal axis of the beams, being caused mainly by the bending effect.

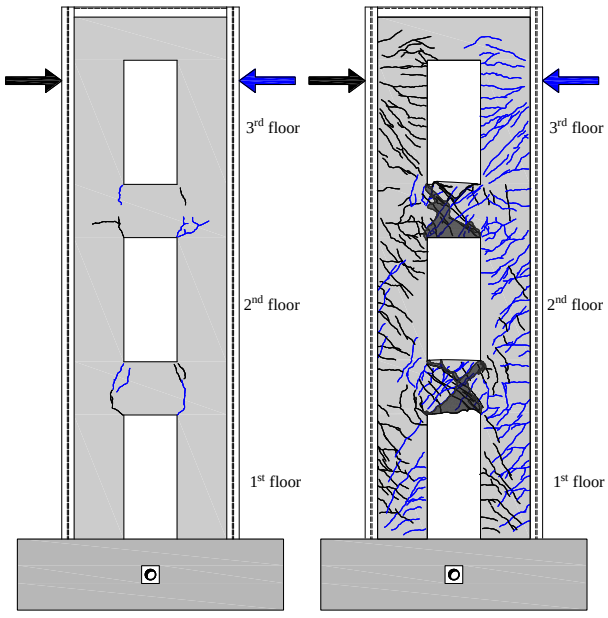


Figure 7. Cracks propagation and local damages recorded

Afterwards, increasing the rotation demand at the base of the wall, reaching the total drift of θ=0,35% new inclined cracks at 35-45° were spread and marked on the lateral surface of the coupling beams. These cracks started to develop on the centre of the beams and were crossing their entire length, being associated to the shear stresses. On the edges of the specimen, horizontal cracks were recorded, at the steel-concrete interface,

indicating the fact that the shear connectors are active and bear the local stresses transferred between structural steel profiles and reinforced concrete web panel. The seismic behaviour of the wall was symmetric on both loading directions. The specimen reached the peak lateral load of 271,6 kN when the total drift was θ=1,47%. At this level of lateral displacement, the horizontal coupling beams were intersected by widely dense diagonal cracks which measured in opening more than 0,30 mm and marked by the crushing of the compressed concrete in the edges. The vertical piers were intersected by inclined shear cracks on the hight of the specimen, but no significant damages were observed at the end of the test (Figure 8). The failure of the steel-concrete composite wall was triggered by the coupling beams which developed an extremely brittle failure mode governed by the shear forces, characterized by the spalling of the compressed concrete cover and by the yielding of vertical stirrups. The failure modes of the coupling beams over the 1st floor and the 2nd floor are illustrated in Figure 9 and in Figure 10.

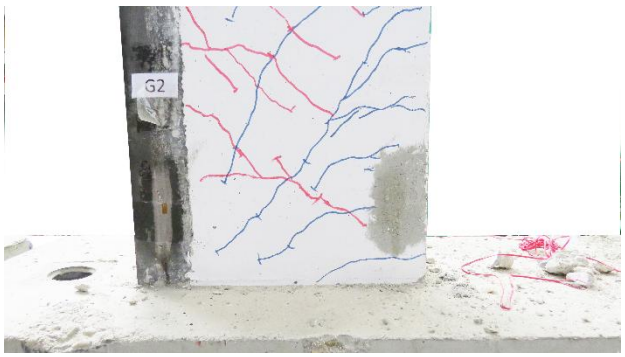


Figure 8. Left pier over the encasement level - final stage

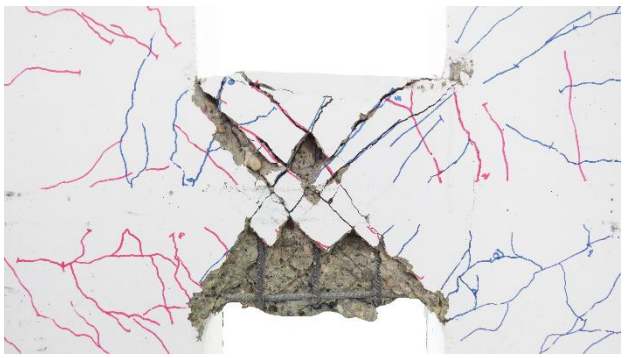


Figure 9. Failure mode of the coupling beam over the 2nd floor

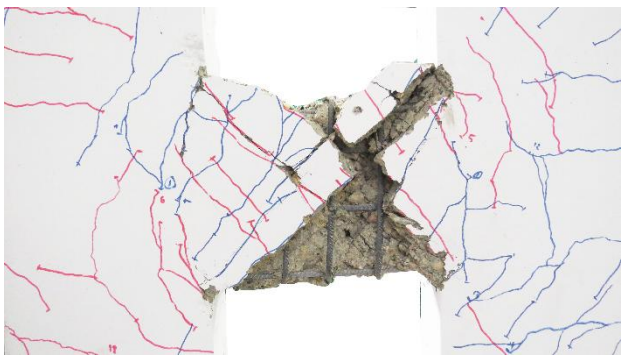


Figure 10. Failure mode of the coupling beam over the 1st floor

3.2 Hysteretic performance of the specimen

The hysteretic curve recorded during the experimental test of the composite wall is presented in Figure 11. The specimen developed a low-dissipative seismic behaviour without significant plastic deformations recorded until the ultimate failure occurred. The main cause for this aspect can be attributed to the coupling beams whose seismic behaviour were governed by shear forces and developed a low deformation capacity under cyclic lateral loads. The peak lateral load recorded on the hysteretic curve in the positive direction of loading was 271,6 kN and in the negative 266 kN, the behaviour being relatively symmetric.

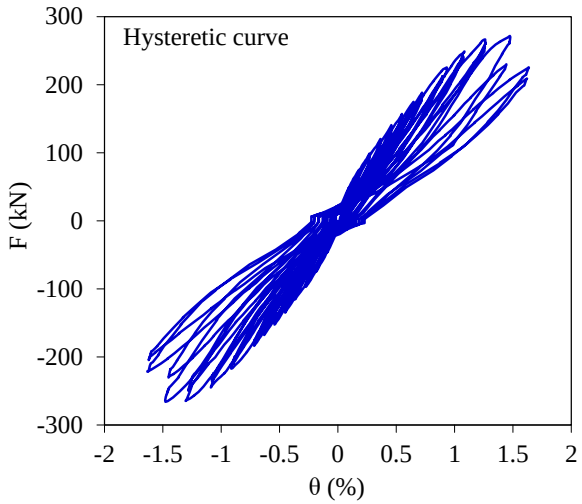


Figure 11. Hysteretic curve of the tested specimen

3.3 Stiffness degradation

The lateral stiffness degradation of structural elements subjected to cyclic lateral loads is another seismic key factor that define his seismic performance. For the tested specimen, the stiffness degradation is illustrated in Figure 12. The initial lateral stiffness in the first cycle of lateral loading was K_i=18,27 kN/mm. Following the curve, it can be said that in the first four cycles of lateral loading, the specimen recorded a significant loss in lateral stiffness, until diagonal cracks were developed on the lateral surface of the reinforced concrete coupling beams. Once these cracks were initiated, the stiffness degradation became almost linear between the subsequent loading cycles.

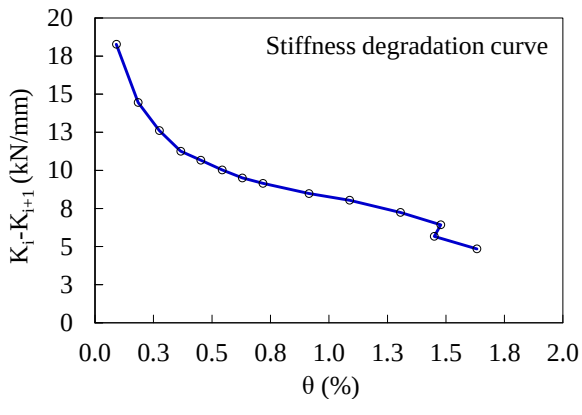


Figure 12. Stiffness degradation of the tested specimen

3.4 Strain analysis

The state of stresses and local deformations developed at each step of loading for structural steel profiles embedded in the edges of the composite wall, was monitorized by four strain gauges denoted G1-G4 were glued on both flanges of the steel profiles over the encasement level in the beam foundation. In Figure 13 is shown the maximum strain ε_s [‰] recorded by the strain gauge G2 during the experimental test, in the positive loading direction. It should be noted that at the peak lateral load, the stresses developed at the base of the wall in the steel profiles have not reached the yielding limit of the S460 steel grade. This aspect was also confirmed by the lack of damage and plastic deformations localized at the base of the vertical piers during the experimental test as shown in Figure 8.

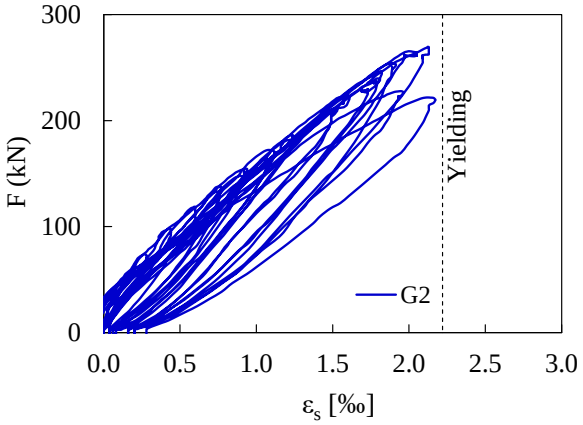


Figure 13. Strain measure by G2

4. FINITE ELEMENT ANALYSIS AND NUMERICAL MODELLING

To validate and verify the experimental results, a push-over finite element analysis using ATENA 3D Engineering (Advanced Tool for Engineering Nonlinear Analysis) software developed by Cervenka Consulting (Cervenka, 2017) was performed. The software is dedicated in evaluating and simulating the real behaviour of concrete and reinforced concrete structures, including the concrete cracking, crushing, and yielding of the steel reinforcements. In Figure 14 the 3D view of the full model is shown. The approached numerical model covers the overall dimensions of the composite wall, the cross-section arrangements, the boundary, and the loading conditions. The displacement control mode was adopted in the nonlinear analyses. The hysteretic envelope curve, the stiffness degradation and the strain analysis recorded numerically are compared with the experimental results.

4.1 Numerical model and boundary conditions

More than eight macroelements were used to construct the numerical model. The connection between the macroelements was considered perfectly rigid being automatically generated by the software. Two additional plates of 30 mm thickness were defined to avoid stress concentrations in points where the vertical and horizontal loads were considered. To simulate the lab foundation support of the wall during the experimental test, a nonlinear surface spring was attached on the bottom side of the beam foundation as can be seen in Figure 14. This resort was infinite rigid in compression and inactive in bearing the negative translations. These translations were restrained by another surface spring characterized by the initial stiffness K=2500 MPa, that was attached to the macroelement that simulate the additional stiff steel beam over the beam foundation as can be seen in Figure 6. This spring simulate the constraints generated by the steel rods that successfully anchored the wall into the rigid floor of the laboratory during the tests. The out of plane displacements and the in-plane displacements of the beam foundation were restrained by using line supports infinite rigid. No geometrical imperfections were considered at modelling. The intensity of the axial force, the top displacement and the state of stresses were recorded during the nonlinear analyses using monitoring points correlated with the position of the displacement transducers or strain gauges glued on the steel profiles based on the experimental stand setup.

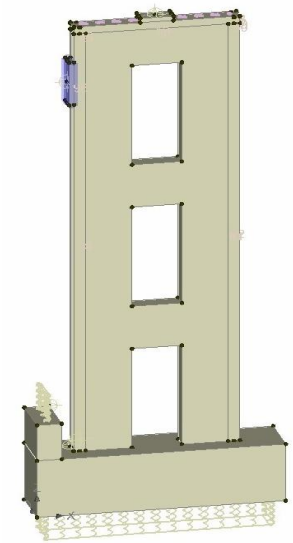


Figure 14. FEM 3D model – perspective view

4.2 Modelling of steel reinforcements

Each bar of the steel reinforcements embedded in concrete was modelled independently as discrete linear elements. The stirrups were modelled without hooks with all the branches interconnected. The bond between the reinforcements and the surrounded concrete was assumed to be perfect, generated automatically by the software. The buckling effect of the compressed bars was neglected. The material law for reinforcements was used to model the behaviour of the in tension and in compression, neglecting the shear stiffness of the bars.

4.3 Materials

The standard “CC3DNonLinCementitius2” SBETA material was used to simulate the nonlinear behaviour of the concrete. The material model includes the following effects: nonlinear behaviour in compression, failure of concrete in tension, cracks propagation, stiffness reduction of concrete in tension after cracking. The material law has included more than 20 parameters which define the overall nonlinear behaviour of concrete, being automatically calculated based on the concrete cubic strength determined experimentally f_{cu}. To simulate the behaviour of the concrete strength class C30/37 the value of the nominal cubic strength f_{cu}=49,23 MPa was considered in the

current analysis. To model the behaviour of the structural steel profiles, the material model "3D Steel Bilinear Von Mises" which incorporates the Von Mises failure criterions was used. The material model simulates the elastic and plastic behaviour of steel in tension and compression based on a bilinear stress-strain law. The following parameters were considered in the analysis to simulate the behaviour of the structural steel: material density ρ=7850 kg/m^3; elasticity modulus E=200 GPa; Poisson ratio ν=0,3; yielding limit σ_y=445 MPa; hardening modulus H=2100 MPa. The Bauschinger effect was also taking into consideration, by using the standard values of the cycling parameters defined automatically by the software. For the reinforcements a multilinear stress-strain law was defined following the stress-strain curve in tension. For the additional steel plates, the "3D Elastic Isotropic" material law was used considering the elasticity modulus E=210000 MPa and the Poisson ratio ν=0,3.

4.4 Discretization and analysis

The 3D isoparametric, quadratic, solid "CCIsoTetra" finite elements were used for FE mesh. The global element size of the finite elements for concrete macroelements was 10 cm while for the structural steel profiles partially embedded in the edges was 5 cm. These dimensions of the mesh were considered to reduce the time for analysing the numerical model. For reinforcements, truss elements "CCIsoTruss" were used at discretization.

4.5 Numerical results – backbone curve

In Figure 15 are illustrated for comparative study the hysteretic curve recorded experimentally and the push-over backbone curve resulted by performing the numerical analysis. The numerical simulation follows with an increased accuracy the low-dissipative seismic behaviour of the experimentally tested composite steel-concrete shear wall. Moreover, the brittle failure mode characterized by the sudden drop of the bearing capacity on the hysteretic curve, is also recorded and captured by the numerical model in the analysis.

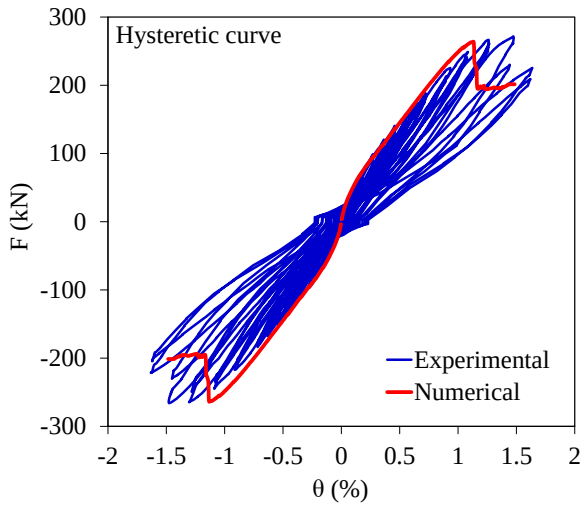


Figure 15. Experimental (hysteretic curve) versus numerical backbone curve of the CSRCW-21-CO specimen

In addition, in terms of peak lateral load, no significant difference was recorded between the numerical and experimental results. The composite wall in the positive direction of loading developed the maximum bearing capacity of F_{exp}=266 kN while numerically on the backbone curve, the maximum lateral load recorded was F_{num}=263 kN. It can be said that the approached numerical model shows a very good agreement to the experimental results, with a divergence less than 1%.

4.6 Numerical results – stiffness degradation

A good correlation between the experimental and numerical results exists also by comparing the stiffness degradation curves presented in Figure 16. The simplified boundary conditions and the material laws considered in the numerical analyses, for the supports and the loading conditions of the specimen, simulated well the arrangements of the experimental stand setup during the analysis. The initial stiffness of the wall in the first cycle of lateral loading was confirmed also by the numerical analysis, with a divergence less than 2% ($K_{i,num}$=18,14 kN/mm).

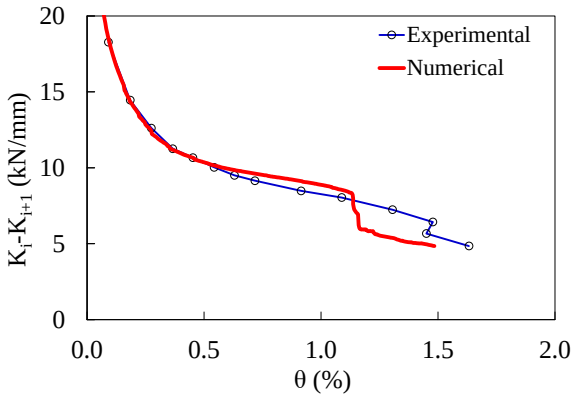


Figure 16. Stiffness degradation – experimental versus numerical curves

4.7 Numerical results – strain analysis

Based on the experimental results the yielding limit of the structural steel profiles embedded in the edges of the composite wall wasn't reached by the tensile stresses. The strains recorded by the strain gauges were less than 2,20 ‰. This aspect was validated by the numerical model after isolating the Von Mises stresses integrated on the cross section of the steel profiles at the base of the wall when the peak lateral load was reached, as can be seen in Figure 17. The maximum tensile stresses are less than 460 MPa.

4.8 Numerical results – local damages

The failure of the specimen was triggered by the coupling beams which failed brittle in shear. By isolating the equivalent plastic strain in compression on the numerical analysis the most damaged elements when the wall reached the peak lateral load were the horizontal beams. In Figure 18 is clear indicated that the vertical piers were insignificantly damaged confirming the observations triggered during the experimental tests.

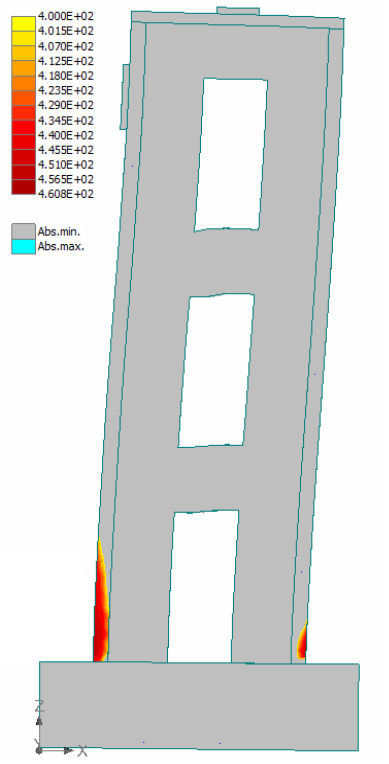


Figure 17. Von Mises stresses isolated on the steel profiles

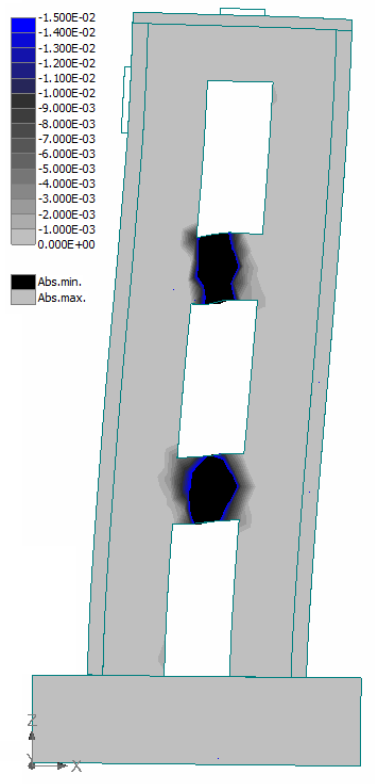


Figure 18. Equivalent plastic strain in compression

4.9 Structural solutions to improve the seismic behaviour.

The numerical analyses were extended furthermore to investigate other possibilities to increase the seismic performance of the composite steel-concrete shear wall. The first solution was to consider additional steel plates of 5 mm thickness in the cross section of the coupling beams and to connect them perfectly rigid with the steel profiles embedded in the edges. The performance obtained subsequently was then compared with the initial seismic performance of the specimen and illustrated in Figure 19. These plates significantly modified the behaviour of the specimen, by increasing the deformation capacity and the bearing capacity.

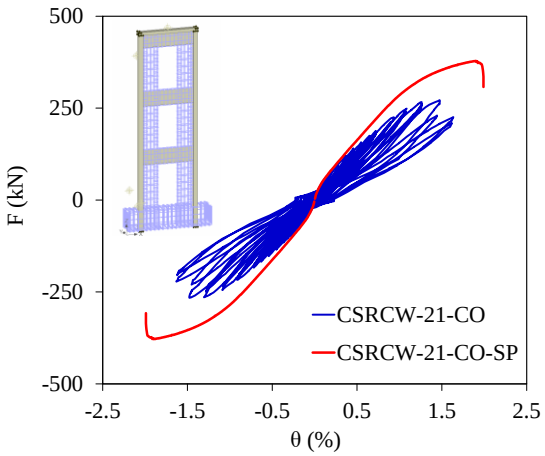


Figure 19. Comparison of tested CSRCW-21-CO hysteretic loop and numerical CSRCW-21-CO-SP backbone curve

The second solution was to design and to reinforce the coupling beams using diagonal steel bars of 12 mm diameter. The steel bars were defined with the same yield strength as the other reinforcements in the design process of the wall. In Figure 19 the numerical results are presented. The diagonal reinforcement increased the bearing capacity and the ductility of the wall with more than 37%.

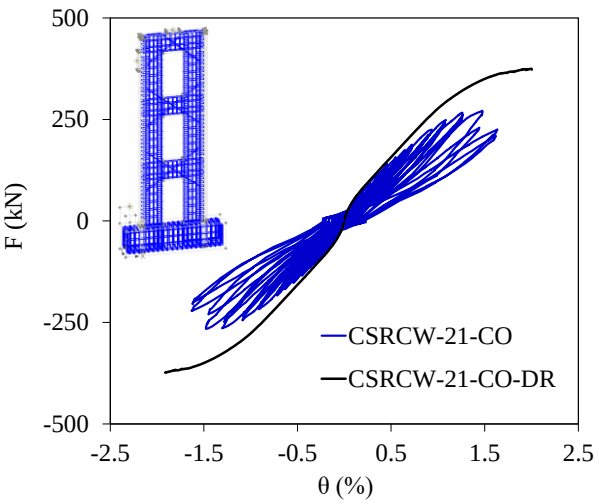


Figure 19. Comparison of tested CSRCW-21-CO hysteretic loop and numerical CSRCW-21-CO-DR backbone curve

5. CONCLUSIONS

This research aimed to study the seismic behaviour of the hybrid/composite steel-concrete shear wall with centred openings. The local damages, cracks development, hysteretic performance and strain analyses were discussed and presented. The following conclusions could be drawn based on the experimental observations and on the numerical analysis:

- The specimen developed a low-dissipative seismic behavior being coupled by conventional reinforced concrete coupling beams. The horizontal beams were governed by shear and failed in a brittle failure mode without dissipating a high amount of hysteretic energy.

- The numerical model predicts very well the seismic behavior and performance of the tested specimen with a divergence of less than 1% in terms of bearing capacity and 2% in lateral stiffness.

- Additional steel plates or diagonal cages can be used to reinforce the coupling beams in the design process of the walls to suppress the brittle failure modes in shear and to increase the deformation capacity of the overall structural system.

6. ACKNOWLEDGEMENTS

This paper was financially supported by the Project "Network of excellence in applied research and innovation for doctoral and postdoctoral programs / InoHubDoc", project co-funded by the European Social Fund financing agreement no. POCU/993/6/13/153437.

References

Dan D., Fabian A., Stoian V., 2011. Nonlinear behavior of composite shear walls with vertical encased profiles. *Engineering Structures*, 10, pp. 2794-2804.

Olabi M. N., Caglar N., Kisa M. H., Yuksel S. B., 2021. Numerical study on the response of composite shear walls with steel sheets under cyclic loading. *Journal of Building Engineering*, 34, p. 102069.

Kisa M. H., Yuksel S. B., Caglar B., 2021. Experimental study on hysteretic behavior of composite steel shear walls with steel sheets. *Journal of Building Engineering*, 33, p. 101570.

Li G., Pang M., Li Y., Li L., Sun F., Sun J., 2019. Experimental comparative study of coupled shear wall systems with steel and reinforced concrete link beams. *The Structural Design of Tall and Special Buildings*, 28(18).

Zhang L., Du W., Zhu B., 2021. Quasi-static testing and numerical simulation study on seismic performance of reinforced concrete core wall with embedded steel frame under sequentially bidirectional loading. *Soil Dynamics and Earthquake Engineering*, 148, p. 106847.

Liu M., Yuan G., Shu Q., Zhang Y., Lu L., 2023. Experimental and numerical investigation on the seismic behaviors of RC shear walls with multiple post-openings before and after strengthening by steel plates. *Engineering Structures*, 279, p. 115552.

Hu L., Feng P., Lin H., Yang J. Q., Qiang H., 2021. Seismic performance of composite shear walls with embedded FCCCs in boundary elements. *Composite Structures*, 257, p. 113126.

Labibzadeh M., Salehnia A., Hossain K. M. A., Jing D. H., 2021. Performance of Composite Shear Walls Subjected to In-plane Cyclic Loading – A Numerical Parametric Study. *Periodica Polytehnica Civil Engineering*.

Ma Z., Wu Y., Wang X., Zhu J., 2023. Seismic behavior of steel plate and reinforced concrete composite wall coupled to steel side columns. *Journal of Building Engineering*, 65, p. 105820.

Kim H. J., Park H. G., 2023. Flexural test for steel-concrete composite walls with steel U-Section boundary element. *Journal of Building Engineering*, 66, p. 105824.

Červenka V., Červenka J., 2017. ATENA Program Documentation - Part 2-2 - User's Manual for ATENA 3D. Červenka Consulting, Prague, Czech Republic.

Wu Y., Fan S., Guo Y., Duan S., Wu Q., 2023. Experimental study and numerical simulation on the seismic behavior of diagonally stiffened stainless steel plate shear walls under low cyclic loading. *Thinn-Walled Structures*, 182, p. 110165.

Li J., Chen L., Wang X., Li F., 2022. Study and numerical analysis on seismic performance of concrete U-shaped shear wall. *Advanced in Materials Science and Engineering*, 2022, pp. 1-21.

Fu Y., Fan G., Tao L., Yang Y., Wang J., 2022. Seismic behavior of prefabricated steel reinforced concrete shear walls with new type connection mode. *Structures*, 37, pp. 483-503.

Phan, D. H., Lin K.C., Phan H.T., 2022. Numerical simulation of full-scale square concrete filled steel tubular (CFST) columns under seismic loading. *Modern Mechanics and Applications*.

Javadi M., Saavedra Flores E. I. S., Yanez S. J., Avudaiappan S., Pina J. C., 2023.

Zhang X., Zhou G., Li S., Zhang F., Zhang S., 2022. Experimental and numerical study on seismic behavior of prestressed concrete composite shear wall. *Engineering Structures*, 266, p. 114546.

Eurocode 4: Design of composite steel and concrete structures: Part 1-1: General rules and rules for buildings, 2004.